Atmos. Chem. Phys. Discuss., 9, 23955–23986, 2009
www.atmos-chem-phys-discuss.net/9/23955/2009/

Atmospheric Chemistry and Physics Discussions

This discussion paper is/has been under review for the journal Atmospheric Chemistry and Physics (ACP). Please refer to the corresponding final paper in ACP if available.

Size-resolved aerosol water-soluble ionic compositions in the summer of Beijing: implication of regional secondary formation

S. Guo[1], M. Hu[1], Z. B. Wang[1], J. Slanina[1], and Y. L. Zhao[2]

[1]State Key Joint Laboratory of Environmental Simulation and Pollution Control, College of Environmental Sciences and Engineering, Peking University, 100871 Beijing, China
[2]Department of Environmental Science, Policy and Management, University of California, 94720 Berkeley, CA, USA

Received: 29 July 2009 – Accepted: 3 November 2009 – Published: 11 November 2009

Correspondence to: M. Hu (minhu@pku.edu.cn)

Published by Copernicus Publications on behalf of the European Geosciences Union.

Abstract

To characterize aerosol pollution in Beijing, size-resolved aerosols were collected by MOUDIs during CAREBEIJING-2006 field campaign at Peking University (urban site) and Yufa (upwind rural site). Fine particle concentrations ($PM_{1.8}$ by MOUDI) were 99.8±77.4 $\mu g/m^3$ and 78.2±58.4 $\mu g/m^3$, with $PM_{1.8}/PM_{10}$ ratios of 0.64±0.08 and 0.76±0.08 at PKU and Yufa, respectively, and secondary compounds accounted for more than 50% in fine particles. PMF model was used to resolve the particle modes. Three modes were resolved at Yufa, representing condensation, droplet and coarse mode. However, one more droplet mode with bigger size was resolved, which was considered probably from regional transport. Condensation mode accounted for 10%–60% of the total mass at both sites, indicating it must be taken into account in summer. The formation of sulfate was mainly attributed to in-cloud or aerosol droplet process (PKU 80%, Yufa 70%) and gas condensation process (PKU 14%, Yufa 22%). According to the thermodynamic instability of NH_4NO_3, size distributions of nitrate were classified as three categories by RH. The existence of $Ca(NO_3)_2$ in droplet mode indicated the reaction of HNO_3 with crustal particles was also important in fine particles. Linear regression gave a rough estimation that 69% of the PM_{10} and 87% of the $PM_{1.8}$ at PKU were regional contributions. Sulfate, ammonium and oxalate were formed regionally, with the regional contributions of 90%, 87% and 95% to $PM_{1.8}$. Nitrate formation was local dominant. In summary regional secondary formation led to aerosol pollution in the summer of Beijing.

1 Introduction

Beijing is the capital and a major metropolis of China with the resident population of over 16 mill (NBSC, 2009a). With the rapid economic development, large energy consumption (4.7 mill tons of coal in 2008, NBSC, 2009b) and increase of vehicles (10–15% per yr, NBSC, 2009b), Beijing has led to air pollution problems. Additionally, Bei-

jing's dustpan shaped topography does not favor air pollution diffusion. Great efforts have been made by Beijing EPB to control primary emission. As a result, SO_2 and NO_2 have met China National Air Quality Standards. However, particles and O_3 have become the major air pollution problems, and the presence of regional and secondary pollution in cities has been recognized recently. It is a serious environmental challenge for China to solve these problems (Shao et al., 2006).

Many studies on chemical compositions of PM_{10} and $PM_{2.5}$ in Beijing have been reported since last few years (He et al., 2001; Yao et al., 2002; Yang et al., 2005; Sun et al., 2006). But the integrated particle compositions can not well characterize the secondary formation process. Size distributions of aerosol water-soluble ionic compositions can help to understand aerosol transformation, transport, and fate. While, only a few studies focused on particle size distributions in Beijing (Yao et al., 2003; Hu et al., 2005a; van Pinxteren, 2009). Moreover, most of previous studies in Beijing were single-site measurements and concentrated on the urban area of Beijing. Model studies on characterizing regional particle pollution of Beijing area are available (Wang et al., 2008), but very few experimental validations were given (Han et al., 2005). It's even rare to quantify the regional component of urban aerosol (Jia et al., 2008). Thus it's necessary to study the size distributions of the secondary aerosols to understand their formation pathways in the regional scale in Beijing.

In this study size-resolved samples were collected by Two Micro-Orifice Uniform Deposit Impactors (MOUDI) at an urban site (Peking University, PKU) and an upwind rural site (Yufa) simultaneously. The size-resolved characteristics of particle mass and chemical compositions were investigated to explore possible formation pathways of secondary compounds and estimate the regional particle contribution.

2 Experiment

MOUDI-110 (10 stages, MSP Corporation, USA) and MOUDI-100, (8 stages, MSP Corporation, USA) were used to sample size-segregated aerosols at PKU and Yufa,

respectively during CAREBEIJING-2006 summer intensive field campaign. The sampling flow rate was 30 L/min, and the 50% cut points of MOUDI-100 were as follows: 10, 5.6, 3.2, 1.8, 1.0, 0.56, 0.32 and 0.18 μm. MOUDI-110 has two more stages with the cut points of 0.1 and 0.056 μm. PKU, the urban site (39° 59′ 21″ N, 116° 18′ 25″ E), was on the roof of an academic building (about 15 m above the ground level) on the campus of Peking University in the northwestern of Beijing. There were no obvious emission sources nearby except two major roads, 150 m to the east and 200 m to the south. Yufa, the rural site (39° 30′ 49″ N, 116° 18′ 15″ E), was about 53 km to the south of PKU, on top of a building (about 20 m above the ground level) at the campus of Huangpu College. Around the site was nothing but farm land and residential area.

Three-period MOUDI samples (morning, afternoon and night) were collected: morning (07:00–11:30, marked A), afternoon (12:00–18:00, marked P), night (18:30–06:30, marked N). The afternoon sampling periods matched the diurnal O_3 peak. In some days, daytime was not divided to ensure that the mass was enough for analysis (marked AP). Teflon filters (Whatman Inc. Clifton, NJ, USA) were used. Before and after sampling, the filters were weighed in Peking University's clean room after 24 h conditioning under constant temperature (20±1°C) and RH (40±3%). The filter preparation and sampling method were the same as Hu et al. (2005a).

Totally 28 and 45 sets of samples were collected at PKU and Yufa, respectively. After sampling the filters were put back in their own Petri dishes, and stored in a refrigerator. During transport to the analysis laboratory they were kept in ice boxes.

Totally five kinds of cations (Na^+, NH_4^+, K^+, Mg^{2+}, Ca^{2+}), four kinds of anions (F^-, Cl^-, NO_3^-, SO_4^{2-}), and three kinds of low molecular weight water soluble organic compounds (formate, acetate, oxalate) were analyzed. The analysis methods were the same as Hu et al. (2005b). Field and laboratory blanks were analyzed using the same method, and the blank concentrations were all below the detection limits. For inter-comparison of two MOUDIs, please see supplement material (http://www.atmos-chem-phys-discuss.net/9/23955/2009/acpd-9-23955-2009-supplement.pdf).

3 Results and discussion

3.1 PM_{10} concentrations and definitions of "polluted" and "clean" episodes

MOUDI does not have a 2.5 μm cut point, so the diameter of 1.8 μm is defined as the cut point to split fine and coarse particles in this study. Therefore, $PM_{1.8}$ and $PM_{1.8-10}$ presented fine and coarse particles. 24 h average PM_{10} concentrations were 171.5±91.4 $\mu g/m^3$ at PKU and 111.6±73.2 $\mu g/m^3$ at Yufa, respectively (Table 1). In average, both fine and coarse particle concentrations at PKU were higher than those at Yufa. These years $PM_{1.8}$, PM_{10} and $PM_{1.8}/PM_{10}$ all increased, compared with the results in summer of 2001, 2002 and 2006, indicating the fine particles have become the major component of PM_{10}, and determined the fluctuation of PM_{10}. In the year 2002 and 2006, secondary compounds ($SO_4^{2-}+NO_3^-+NH_4^+$) compose more than half of the fine particle mass, suggesting secondary particle pollution had become more and more important these years.

"Polluted" and "clean" episodes are defined based on particle mass concentrations, SORs (molar ratio of the particulate sulfate to the total sulfur $SO_4^{2-}+SO_2$) and meteorological conditions. Totally four "polluted episodes" , that is, 18–19 August, 24–25 August and 2–3 September, 6–7 September are defined (Fig. 1: P1–P4), with high PM_{10} concentrations (>100 $\mu g/m^3$), stagnant meteorological conditions (wind speed <1 m/s), high temperature (>30°C) and RH (>70%). The SORs during the polluted episodes were higher than 0.3. Two "clean episodes" were observed during 20–21 August and 4 September (Fig. 1: C1–C2, samples were not collected on 4 September PKU for technical reason), with strong wind (max wind speed >4 m/s), high temperature (>30°C) but low RH (<50%). The SORs during the clean episodes were lower than 0.2.

NOAA's HYSPLIT4 trajectory model (www.arl.noaa.gov/hysplit.html) was used to calculate 24 h backward trajectories of the different air mass origins for different episodes (Fig. 2). The backward trajectories of polluted episodes came from the

ACPD
9, 23955–23986, 2009

surrounding area of Beijing (mainly from south), and the paths were short because of low wind speed. The backward trajectories of clean episodes originate mostly from far north of Beijing, where the air is relatively clean. The strong wind took the clean air to scavenge and dilute the polluted air in Beijing. For general description of gaseous pollutants and meteorological conditions during two types of episodes, please see supplement material (http://www.atmos-chem-phys-discuss.net/9/23955/2009/acpd-9-23955-2009-supplement.pdf).

All in all, in the summer of Beijing fine particles were dominant in PM_{10}. The stagnant atmosphere favored secondary transformation and pollution accumulation. The precipitation or strong wind from north interrupted the pollution accumulation process by scavenging and dispersions. Thus the "polluted" and "clean" episodes occurred alternately.

3.2 Size distributions of mass and ionic compounds

3.2.1 Resolving size distribution modes

Ambient aerosol distribution is characterized by a number of modes. Usually, aerosol mass is dominated by bimodal distribution, the accumulation mode and coarse mode. In some cases the accumulation mode consists of two overlapping sub-modes: the condensation mode and the droplet mode. Aerosol mode distribution reflects the origin of aerosol. For instance, the condensation sub-mode is the result of growth of ultrafine particles by coagulation and vapor condensation. The droplet sub-mode was formed by in-cloud process or aqueous reaction. Thus, it is helpful to distinguish the mode distribution so as to track the formation path for secondary composition. Factor analysis techniques are good methods to resolve the overlapping peaks (Frenich et al., 2000), among which the positive matrix factorization (PMF) model has recently been successfully applied to the resolution of different particle modes (Kim et al., 2004; Huang et al, 2006). Totally 196 sets (7 species×28 samples) sets and 315 sets (7 species×45 samples) of size distribution data were generated at PKU and Yufa, respectively, with 7

species of mass and 6 measured chemical compositions (SO_4^{2-}, NO_3^-, oxalate, NH_4^+, Ca^{2+} and K^+). PMF analysis was performed on these data at PKU and Yufa separately with the number of factors fixed at three or four according to the measured size distribution.

PMF is a multivariate factor analysis tool that decomposes a matrix of speciated sample data into two matrices (factor contributions and factor profiles). In the case of this study, MOUDI size distribution data can be viewed as a data matrix **X** of i by j dimensions, in which i number of samples and j number of particle size bins (MOUDI stages). PMF is to identify a number of factors p, the MOUDI stage profile f of each source, and the amount of mass g contributed by each factor to each individual sample (see Eq. 1):

$$x_{ij} = \sum_{k=1}^{p} g_{ik} f_{kj} + e_{ij} \quad (1)$$

where e_{ij} is the residual for each sample/species.

As a result, the concentration of each MOUDI stage was decomposed into three or four factors due to the different sources. In other words, each mass size distribution (total mass or mass of each chemical composition) of every single sample was decomposed into three or four distributions (factors). Average size distributions for each factor are calculated by averaging all the same stages in one factor (e.g. the resolved concentrations in all 0.56–1 μm stages of factor 1 are averaged to get the average concentration of 0.56–1 μm for factor 1). The sum concentration of all stages in one factor is the contribution of this factor to total mass concentration, and lognormal fit was used to get each factor's mass medium aerodynamic diameter (MMAD). The factors are named after well known particles submodes (condensation mode, droplet mode and coarse mode) according to their MMADs.

The measured and resolved average size distributions were showed in Fig. 3. For rural Yufa site, apparent three modes were resolved by PMF with at 0.4, 0.8, and 5.7 μm, corresponding to the condensation mode, droplet mode, and coarse mode,

respectively (Fig. 3). The results were similar to those of the rural aerosols in Shenzhen, China (Huang et al., 2006). While for PKU, four modes of particle mass were resolved, with the MMADs at 0.4, 0.8, 1.4 and 5.7 μm, corresponding to the condensation mode, droplet mode-1, droplet mode-2, and coarse mode, respectively. One more droplet mode with bigger size was resolved at urban site. Three or four modes mass distributions will be discussed later.

3.2.2 Size distributions at Yufa

The measured mass size distribution showed bimodal size distributions with the peaks at the stages of 0.56–1 μm and 3.2–5.6 μm at Yufa (Fig. 4a-2), which was consistent with the previous study in Beijing (Yao et al., 2003). The PMF model resolved three modes of condensation mode, droplet mode and coarse mode. The PMF model separated the condensation and droplet mode based on MOUDI measured results, and the condensation mode accounted for 10%–60% of the total mass, indicating the condensation mode, which was neglected by previous study, was also important in summer of Beijing, and should be taken into account.

During the polluted episodes droplet mode was the dominant mode, and the percentage of this mode in total mass did not vary a lot, with 54%, 51% and 49% in the morning, afternoon and night, respectively (Table 2). Correspondingly, the condensation mode accounted for 24%, 27% and 27% of the total mass, respectively. In contrast during the clean episodes under the dry and cool weather condition, the droplet mode particles did not favor to form due to lack of water vapor in the atmosphere. Thus, the droplet mode was no longer the major mode instead of the coarse mode and the condensation mode with the average fractions of 47% and 42% in the total mass, respectively.

The measured sulfate, nitrate and ammonium all showed bimodal size distribution with two peaks at 0.56–1 μm and 3.2–5.6 μm (Fig. 4), and they were all resolved into three modes by PMF model. However, these compounds had different diurnal variations and bimodal shapes. Sulfate had a major fine mode peak and a small coarse

mode peak. The highest concentration occurred in the afternoon, because of the strong production process. The PMF model results exhibited the same diurnal variation, but resolved tri-modal distribution, a predominant droplet mode, a small condensation mode, and a small coarse mode. The PMF results also showed that although the concentration of sulfate varied with time, the percentage of each mode did not change much, which means the distribution did not change with time. However, nitrate showed a different diurnal variation from sulfate, with highest concentration at night and lowest in the afternoon, and it had a larger coarse mode with the fractions of 26%, 63% and 19% in the morning, afternoon and night, respectively. Moreover, the nitrate distribution varied with time. In the morning and night samples, droplet mode was the dominant mode accounting for 58% and 64% of the total nitrate, but in the afternoon coarse mode became the major mode. Ammonium had a similar bimodal shape to sulfate but showed no apparent day-night variation, and the highest ammonium concentration occurred in the morning.

Oxalate was the most abundant dicarboxylic acid, accounting for 0.4% in PM_{10} and 0.5% in $PM_{1.8}$. Its size distributions were similar to those of sulfate. Formate and acetate can be measured in most of the samples (0.2% and 0.2% in $PM_{1.8}$), and they were found in both fine and coarse particles, with 55% and 58% in the fine mode, respectively.

3.2.3 Size distributions at PKU

At PKU the size distributions of mass and major ionic composition were similar to those at Yufa, but there were several differences. 1) Four modes were resolved by PMF, with one more droplet mode with bigger size. 2) The fine particle peak for morning and afternoon were the same as Yufa at 0.56–1 μm, while at night the peak "shifted" to bigger size of 1–1.8 μm, indicating the resolved droplet mode with bigger size was reasonable. 3) Corse mode contributed more at PKU than that at Yufa, due to more resuspended dust by traffic and more construction works before Olympics.

The first two differences will be discussed together here. Some researches have also

measured this peak "shift". Anlauf et al. (2006) considered the shifts of the fine mode peaks at night were due to some aqueous-phase production. The shifts may also be simply due to increased water content at the high values of relative humidity. Liu et al. (2008) also measured large amount of particles in the stage of 1–1.8 μm at night, and they suggested these particles may be from the hygroscopic growth of particles of 0.56–1 μm. However, these cannot fully explain the bigger size droplet mode particles in this study, because the fine mode peaks did not "shift" to bigger size at Yufa, while the gaseous precursor's concentration, temperature and RH at both sites were all similar.

This study considered these bigger size droplet mode particles were produced and grew during regional transport, and the different upwind conditions of two sites led to the different size distributions. The upwind area of the PKU site was polluted urban area, and when the particles passed through the urban area, they were aged and grew to bigger size. Differently, the upwind area of Yufa was not so polluted (at least within tens of kilometers), and under this condition the particles did not favor to grow up. Evidence is the t-test results showed that during the stagnant south wind days, the bigger size droplet mode moderately correlated with wind speed, and the bigger size droplet mode at PKU correlated with the droplet mode at Yufa with correlation coefficient of 0.74. PMF results could provide more information to explain these particles. Two droplet modes were resolved by PMF, a similar droplet mode as that at Yufa and an extra droplet mode with bigger size. The mass concentrations of the bigger size droplet mode had no significant diurnal variation, and showed no correlation with O_3, indicating the source of these particles was persistent and was less related with O_3 chemistry. Thus, these particles may from in-cloud process of long range transport. However, more strong evidences are still needed to explain this hypothesis.

3.3 Formation of sulfate, nitrate and oxalate

3.3.1 Formation of sulfate

Total sulfate in PM_{10} and SO_2 exhibited similar temporal trend at both sites, with a higher concentration in the daytime (Fig. 5). T-test results exhibited that daytime sulfate was moderately correlated with SO_2 at both sites, but poorly correlated at night. The absence of the nighttime correlation between sulfate and SO_2 suggests the deposition of sulfate was of greater importance than aqueous-phase production during the nighttime. The average SORs during the campaign excluding the clean episodes were 0.42 and 0.46 at PKU and Yufa, respectively. The high values of SOR (>0.1) indicated the conversion had progressed considerably (Ohta et al., 1990). Also the SOR values exhibited distinct diurnal variation, with higher ratios at daytime. The situation during the clean episodes was different. The strong north wind advected cold dry air, and diluted both gaseous and particulate pollutants, the SORs were below 0.2.

PMF-resolved particles of different modes were actually from different sources. For secondary compounds, the different sources means different formation pathways, so PMF results can be used to estimate the contributions of different formation pathways. This estimation needs to meet two restrictive conditions: 1) the component must be mainly from secondary transformation; 2) The formation pathways of the component must be known.

Sulfate can come from both primary and secondary sources. Biomass burning such as wood burning and meat cooking can release particulate sulfate at the size range of about 0.1 μm (Kleeman et al., 1999). Water-soluble K^+ is a good tracer for biomass burning, and the ratios of mass concentrations of K^+ to sulfate are usually larger than one in the biomass burning particles. In this study, the ratios were 0.10±0.06 and 0.11±0.10 at PKU and Yufa, respectively. Moreover, the correlation between K^+ and sulfate in fine particles was poor at both sites. These results indicate that direct sulfate emission by biomass burning could be ignored. Vehicles also emit particulate sulfate, and the Cassiar tunnel measurements of particles indicated a mass ratio of Na^+ to

SO_4^{2-} of about 0.05 (Anlauf et al., 2006). The average ratios for the 0.56–1 μm particles at PKU and Yufa were 0.018 and 0.017, and the ratios would be less considering that sodium was also contributed by other sources. Generally, notwithstanding the large quantities of primary emission, fine mode sulfate mainly came from secondary sources.

Numerous studies have been carried on formation pathway of sulfate, and its formation mechanisms are relatively well understood. Several possible formation processes have been proposed to explain the droplet mode sulfate, including condensation and coagulation of smaller particles, in-cloud processes and the growth of the condensation mode by addition of sulfate and water (aerosol droplet process). The condensation mode sulfate arises from homogeneous gas phase photochemical oxidation of SO_2 followed by gas-to-particle conversion (Seinfeld and Pandis, 1998). The coarse mode sulfate could be attributed to heterogeneous reactions of SO_2 on soil particles (Zhuang et al., 1999). However, the contributions of these formation pathways alter with temporal and spatial variation. Although the previous study has concluded the sulfate was attributed to in-cloud processes in the summertime of Beijing (Yao, et al., 2003), the contributions of different formation pathways have not been quantified yet due to lack of suitable analysis technique.

As a result, in summer of Beijing, droplet mode was dominant, and an average fraction of 80% and 70% was attributed to in-cloud or aerosol droplet process at PKU and Yufa, respectively. Correspondingly, 14% and 22% of the sulfate was attributed to gaseous H_2SO_4 condensation. This result showed the gas-to-particle conversion was also an important formation pathway for sulfate in summer of Beijing.

3.3.2 Formation of nitrate

In-cloud uptake of nitric acid and condensation onto pre-existing particles are two possible pathways to form fine mode nitrates. In this work, fine mode nitrate and sulfate exhibited a good correlation with R^2=0.78 at Yufa, indicating their formation pathways may similar. However, the correlation at PKU was weak with R^2=0.41, suggesting at

PKU the nitrate formation was different from sulfate, so the formation pathway of nitrate at PKU will be discussed in detail below.

The measuring of particle NH_4NO_3 has a lot of artifacts due to its semi-volatility, and this has been known for a long time and has been documented in detail in the literature (Chow, 1995). These artifacts are mainly caused by topological reactions, and evaporation of ammonium nitrate. Topological reactions will be important noticeable if the loading of the filters is high, because nitrate can react with sulfuric acid to form nitric acid, which will lose by evaporation. Thus, more nitrate will be lost if the sampling period is long (e.g. 24 h). The evaporation of NH_4NO_3 could also take place during the sampling, especially when in the afternoon the temperature was high and the humidity is low. Both these aspects could make the filter measurement underestimate the concentrations of nitrate and ammonium. Online instrument with short sampling time can effectively reduce the artifacts, so in this study, particle compositions SO_4^{2-}, NO_3^- and NH_4^+ were also measured by the on-line aerosol and gas instrument Wet Denuder-SJAC (Steam Jet Aerosol Collector) system (Slanina et al., 2001). Wet Denuder-SJAC can also measure gaseous NH_3 and HNO_3.

Many studies have reported that fine mode nitrate was ammonium nitrate, but the chemistry of coarse mode nitrate in different locations can be diverse, not only NH_4NO_3 but also $NaNO_3$ and $Ca(NO_3)_2$ have been reported (Pakkanen et al., 1996). Basically, the size distribution of nitrate is influenced by the thermodynamic equilibrium of

$$HNO_3(g) + NH_3(g) \longleftrightarrow NH_4NO_3(s,aq) \quad (2)$$

When the $[NH_3]\times[HNO_3]$ is larger than the equilibrium constant Ke′, formed $NH_4NO_3(s,l)$ can be stable. Otherwise nitrate can exist in coarse mode. The equilibrium constant Ke for pure NH_4NO_3 is determined by temperature, ambient RH and the concentrations of $HNO_3(g)$ and $NH_3(g)$. In this study Ke is calculated using the method suggested by Michael (1993). The coexistence of SO_4^{2-} in particles considerably reduces Ke. To determine Ke′ for the $NH_4^+/NO_3^-/SO_4^{2-}$ system, the NH_4NO_3 ionic strength fraction Y was calculated according to Stelson and Seinfeld (1982). Ke′ was

then derived by multiplying Ke with Y.

The equilibrium constant (Ke′) and the measured $[NH_3]\times[HNO_3]$ were calculated by using SJAC data. Figure 6 shows the equilibrium constant (Ke′) as calculated and as measured $[NH_3]\times[HNO_3]$ at PKU during the campaign. Both temperature and relative humidity had great impact on the size distribution of nitrate. However, the variation of temperature was small (22.3~30.1°C), which means very small change of temperature can lead to large change of Ke′. It's difficult to set a critical point of coarse-to-fine mode shifting by using temperature. Three kinds of cases were classified by RH: 1) when the relative humidity was lower than 50%, the red triangles in Fig. 6 are much higher than corresponding blue circles, and the Ke′ values were about one order larger than the measured $[NH_3]\times[HNO_3]$ products. Under this condition, and NH_4NO_3 dissociated and formed coarse mode nitrate by reactions of nitric acid with $CaCO_3$, K_2CO_3 or NaCl. 2) When the humidity was between 50–70%, the measured products were often in the same order compared to Ke′. NH_4NO_3 can partly dissociate, and existed in both fine particles and coarse particles. 3) When the humidity was over 70%, the triangles and circles are close to each other. Sometimes, the measured $[NH_3]\times[HNO_3]$ was even higher than Ke′. This may happen after midnight when the humidity was very high. Under this condition, NH_4NO_3 is found in fine particles. This classification can be validated by measured size distribution results.

At Yufa the nitrate size distributions agreed with the above classification very well. However, the case at PKU site was quite different. In the afternoon, the RH was usually below 50%, but considerable amounts of fine particle nitrate were measured, (Fig. 4c-1), so there must be other cations that combined with nitrate in fine particles besides ammonium. Crustal aerosol like $CaCO_3$ can also react with nitric acid to form $Ca(NO_3)_2$. It was generally assumed that calcium is mainly present in the coarse particles, so these reactions would be only relevant for coarse particles. The calcium in fine particle was seldom investigated in previous studies. However, the results of this study show that 29% of the water-soluble Ca^{2+} was in fine particles. Moreover, K^+ was abundant in fine particles, so it was possible that fine mode nitrate can exist as the form

ACPD
9, 23955–23986, 2009

of $Ca(NO_3)_2$ or KNO_3. The molar ratios of r' and r in stage 0.56–1 μm and 1–1.8 μm were calculated to show that sufficient Ca^{2+}, K^+ and Na^+ is present:

$$r' = \frac{[Na^+] + [K^+] + 2 \times [Ca^{2+}]}{[NO_3^-] + [Cl^-]}, \quad (3)$$

$$r = \frac{[K^+] + 2 \times [Ca^{2+}]}{[NO_3^-]} \quad (4)$$

The weather conditions of 24 and 25 August were different from those of other days, so the discussion below will not include these two days. The calculation results showed that r' ranged from 0.84 to 1.36, and r ranged from 0.74 to 1.43, indicating these cations were abundant enough to combine with nitrate. In addition, the correlation between these cations and nitrate in the afternoon samples was investigated (Table 3). Na^+, K^+ and Ca^{2+} showed good correlation with nitrate, implying in the afternoon samples at PKU, nitrate was of great possibility to exist as $NaNO_3$, KNO_3 and $Ca(NO_3)_2$. Moreover, in the stage of 1–1.8 μm, Ca^{2+} was the most abundant in these three cations, and had best correlation with nitrate, so $Ca(NO_3)_2$ may be dominant in this stage. For the same reason, in the stage of 0.56–1 μm, KNO_3 may be important, although NH_4NO_3 was also probably present in this stage. Assuming all the Ca^{2+} in fine particles was formed as $Ca(NO_3)_2$, about 46% of the fine mode nitrate was attributed to reactions of gas HNO_3 with crustal particles in the afternoon at PKU site. However, this result is overestimated for neglect of the $CaSO_4$ in fine particles. The same calculation was done with the Yufa afternoon samples, and the percentage was about 26%.

The afternoon samples of 24 ans 25 August were special cases. The amounts of the three cations were too low to act as counter-ions for nitrate, the average temperatures during these two sampling periods were below 30 degree and average RH was higher than 60%, indicating that ammonium nitrate was possible dominant form of fine mode nitrate.

In the morning and night samples, there were also probably some $Ca(NO_3)_2$ in fine particles, but the cases were more complicated. NH_4NO_3 in fine particles may be stable or partly disassociated, so it is hard to estimate how much nitrate was formed as $Ca(NO_3)_2$. In conclusion the reaction of HNO_3 with crustal particles was important in both fine and coarse particles, in the summer of Beijing.

3.3.3 Formation of oxalate

Oxalate is typically the most abundant dicarboxylic acid in atmospheric aerosols, and has been found in particle composition in various environments (Narukawa et al., 2003). Oxalate can come from primary emission of vehicle exhausts (Kawamura and Kaplan, 1987), biomass burning (Narukawa et al., 1997) and biogenic activity (Kawamura, 1996). Biomass burning can release oxalic acid, and oxalate correlates well with K^+ in these particles (Narukawa et al., 1999). However, in this study, oxalate had a poor correlation with K^+ (R^2=0.43, PKU; R^2=0.07, Yufa), indicating biomass burning was not a major source of oxalate. Plant leaves do not emit oxalic acid directly, but fatty acids released by plant may be broken down to form oxalic (Kawamura et al., 1996). Biogenic activities in the soil and the roots of plants can also generate oxalic acid (Jones, 1998). So far the formation of oxalate by biological aerosols is not well understood yet. Above all, primary emission was not the main source of oxalate in the summer of Beijing.

Another source of oxalate is from secondary transformation. The condensation mode oxalate is mainly from the photochemical process in the gas phase to form gaseous oxalic acid, followed by its condensation onto existing particles. However, it is impossible for condensation mode oxalate to directly grow up into droplet mode in Beijing, because only at very high RH of 97% (at 25°C), the condensation mode of pure oxalic acid or the mixture of oxalic acid, sulfate and nitrate can grow up into droplet mode by hygroscopic growth (Peng et al., 2001). Thus, it is possible that the condensation mode oxalate-containing particles were activated and became the droplet mode particles after in-cloud or aerosol droplet process in Beijing.

Generally, similar size distributions indicate similar formation processes. The size distributions of oxalate were almost of the same as those of sulfate, and oxalate and sulfate were highly correlated with correlation coefficients of 0.89 and 0.90 at PKU and Yufa, respectively, strongly suggesting that oxalate and sulfate originated from similar atmospheric processes. Many studies have reported the good correlations between sulfate and oxalate (Huang et al., 2006). From the PMF results, 67% of oxalate at PKU and 55% at Yufa were formed by in-cloud or aerosol droplet process. Correspondingly, 19% and 25% were due to gas-particle condensation.

3.4 Assessment of local and regional particulate pollution

Recently, the presence of regional pollution in cities has been recognized. This pollution considers a background whose concentration and variation were within regional scale, and can limit efforts to reduce air pollution in cities. This regional concentration is difficult to quantify, even with transport models (Jia et al., 2008). Various assumptions were given in different studies, basing on which the regional contribution of urban area can be estimated (Han et al., 2005). However, these methods need large quantities of long-term and high resolution data.

A simple method was used in this study to very roughly estimate the regional contribution. Several assumptions were made in this method: 1) The particle concentrations of urban site was only from regional and local contribution. The regional contribution included regional background concentration and regional transport, which in this study contributed very little, and can be considered as a very small constant due to the stagnant weather condition. 2) The particle concentrations at the regional site Yufa can be considered as homogeneous regional background concentration plus local contribution at Yufa which can also be regarded as a small constant due to very few local effects. 3) The particle pollution at two sites had similar variations, and the contribution, which the urban area gives to the regional area, is linear. Under these assumptions,

the urban particle concentration C_{urban} can be present as:

$$C_{urban} = C_{PKU} = R + L = (R_b + R_t) + L = R_b + L + c_0 \quad (5)$$

in which, R, R_b and R_t are regional, regional background and regional transport contribution, and L is local contribution. Due to assumption 1), R_t can be assumed as a constant c_0. According to assumption 2) and 3), R_b equals to C_{Yufa} plus local contribution c_0', and R can be expressed as $b * C_{PKU}$, in which b is the fraction of regional contribution. Thus the Eq. (4) can be transformed to Eq. (5):

$$b * C_{PKU} = C_{Yufa} + c \quad (6)$$

in which c is sum of c_0 and c_0'.

To estimate regional contribution, two steps are needed to do. First, the regional character must be recognized for the component (mass or chemical compositions). Then, linear regression is made to calculate the b value. In this study, the particle concentrations at two sites showed similar trends and were strongly correlated (R^2=0.86 for $PM_{1.8}$, R^2=0.83 for PM_{10}, n=28), this clearly points to the regional character of particle concentrations. By the method above, an average regional contribution of 69% was estimated for PM_{10} and 87% for $PM_{1.8}$. This result was consistent with the study of Jia et al. (2008), in which 70% of the urban PM_{10} concentration was estimated from regional contribution during southerly flow. The offset c was decided mainly by two aspects: local contribution at Yufa and transport contribution at PKU. The positive c value indicates at least regional transport did contribute to urban particle pollution, although the contribution was less than 5%.

The correlation between PKU and Yufa regarding sulfate in $PM_{1.8}$ was good (R^2=0.81, n=28) during stagnant days, suggesting the regional sulfate pollution. The same variation of SORs at two sites also indicated the regional production of sulfate. Using the same estimating method, about 90% of the sulfate in $PM_{1.8}$ at PKU is regional. Oxalate and ammonium were also formed regionally, with average regional contributions of 95% and 87%, respectively.

As mentioned above, nitrates at two sites had different formation pathways, suggesting the formations of nitrate at two sites depended more on local conditions. Moreover, the nitrate in $PM_{1.8}$ showed weak correlation between PKU and Yufa, with R^2=0.34. All these differences indicate that nitrate was formed locally other than regionally.

Because the regional particle pollution is very complicated, and the assumptions of this method have many uncertainties, this method can only give very rough estimation. However, this method is suitable for the case that only short time and low time resolution data are available, and the estimation does not need to be very accurate.

4 Conclusions

In summer of Beijing, the particle concentrations were both high at urban site and rural site. The fine particles have become the major component of PM_{10}, and secondary pollution was more and more important these years. Three modes were resolved at Yufa by PMF model, representing three major sources of particles. However, one more droplet mode with bigger size was resolved, which was considered probably from regional transport, but more evidences were needed to prove this. Condensation mode should also be taken into account for its contribution of more than 1/4 to total mass. The PMF results can be used to quantify the contribution of each formation pathway. As a result, 80% of the sulfate at PKU and 70% at Yufa were due to in-cloud process or aerosol droplet process, and correspondingly 14% and 22% were due to gas condensation process. Oxalate had similar formation pathway as sulfate, with the contributions of 67% at PKU and 55% at Yufa due to in-cloud or aerosol droplet process. Nitrate size distributions were classified as three categories by RH due to the thermodynamic instability of NH_4NO_3. The nitrate in fine particles in the afternoon at PKU was probably $Ca(NO_3)_2$ in stage 1–1.8 μm and KNO_3 in the stage of 0.56–1 μm, indicating the reaction of HNO_3 with soil particles was not only important in coarse particles, but also in fine particles. Linear regression was used to roughly estimate the regional particle contribution. As a result, 69% of PM_{10} and 87% of $PM_{1.8}$ at PKU were re-

gional contributions. Sulfate, ammonium and oxalate were formed regionally, with the regional contributions of 90%, 87% and 95% to $PM_{1.8}$ at PKU. Nitrate formation was local dominant.

Acknowledgement. This work as part of CAREBEIJING 2006 (Campaign of Atmospheric Researches in Beijing and surrounding areas in 2006) were supported by Beijing Council of Science and Technology (HB200504-2, HB200504-6), The National Natural Science Foundation of China (20637020), the National Key Technologies R&D Program in the Eleventh Five-year Plan Period from the Ministry of Science and Technology (2006BAI19B06). The authors would like to thank W. Zhang, D. Chen, Y. Li, J. Gu for their help during the campaign. Thanks to J. J. Schauer, Y. Song and R. Jansen for their suggestions and editing advice.

References

Anlauf, K., Li, S. M., Leaitch, R., Brook, J., Hayden, K., Toom-Sauntry, D., and Wiebe, A.: Ionic composition and size characteristics of particles in the lower Fraser Vellay: Pacific 2001 field study, Atmos. Environ., 40, 2662–2675, 2006.

Chow, J.: Critical review of measurement methods to determine compliance with ambient air quality standards for suspended particulates. J. Air Waste Manage., 45, 320–382, 1995.

Frenich, A. G., Galera, M. M., Vidal, J. L. M., Massart, D. L., Torres-Lapasio, J. R., De Braekeleer, K., Wang, J. H., and Hopke, P. K.: Resolution of multicomponent peaks by orthogonal projection approach, positive matrix factorization and alternating least squares, Anal. Chim. Acta, 411, 145–155, 2000.

Han, L. H., Zhuang, G. S., Yele, S., and Wang, Z. F.: Local and non-local sources of airborne particulate pollution at Beijing. Sci. China Ser. B, 48(3), 253–264, 2005.

He, K. B., Yang, F. M., Ma, Y. L., Zhang, Q., Yao, X. H., Chan, C. K., Cadle, S., Chan, T., and Mulawa, P.: The characteristics of $PM_{2.5}$ in Beijing, China, Atmos. Environ., 35(29), 4959–4970, 2001.

Hu, M., Zhao, Y. L., He, L. Y., Huang, X. F., Tang, X. Y., Yao, X. H., and Chan, C. K.: Mass size distribution of Beijing particulate matters and its inorganic water-soluble ions in winter and summer, China Environ. Sci., 26(4), 1–6, 2005a.

Hu, M., Zhang, J., and Wu, Z. J.: Chemical compositions of precipitation and scavenging of particles in Beijing, Sci. China Ser. B, 48(3), 265, 2005b.

Huang, X. F., Yu, J. Z., He, L. Y., and Yuan, Z. B.: Water-soluble organic carbon and oxalate in aerosols at a coastal urban site in China: size distribution characteristics, sources, and formation mechanisms, J. Geophys. Res., 111, D22212, doi:10.1029/2006JD007408, 2006.
Jia, Y. T, Rahn, K. A., He, K. B., Wen, T. X., and Wang, Y. S.: A novel technique for quantifying the regional component of urban aerosol solely from its sawtooth cycles, J. Geophys. Res., 113, D21309, doi:10.1029/2008JD010389, 2008.
Jones, D. L.: Organic acids in the rhizosphere-a critical review, Plant Soil, 205, 25–44, 1998.
Kawamura, K. and Kaplan, I. R.: Motor exhaust emission as a primary source for dicarboxylic acids in Los Angeles ambient air, Environ. Sci. Technol., 21, 105–110, 1987.
Kawamura, K., Kasukabe, H., and Barrie, L. A.: Source and reaction pathways of dicarboxylic acids, ketoacids and dicarbonyls in Arctic aerosols: one year of observations, Atmos. Environ., 30, 1709–1722, 1996.
Kim, E., Hopke, P. K., Larson, T. V., and Covert, D. S.: Analysis of ambient particle size distributions using UNMIX and positive matrix factorization, Environ. Sci. Technol., 38, 202–209, 2004.
Kleeman, M. J., Schauer, J. J., and Cass, G. R.: Size and composition distribution of fine particulate matter emitted from wood burning, meat charbroiling and cigarettes, Environ. Sci. Technol., 33, 3516–3523, 1999.
Liu, S., Hu, M., Slanina, J., He, L. Y., Niu, Y. W., Bruegemann, E., Gnauk, T., and Herrmann, H.: Size distribution and source analysis of ionic compositions of aerosols in polluted periods at Xinken in Pearl River Delta (PRD) of China, Atmos. Environ., 42(25), 6284–6295, 2008.
Michael, M.: The dissociation constant of ammonium nitrate and its dependence on temperature, relative humidity and particle size, Atmos. Environ., 27A, 261–270, 1993.
Narukawa, M., Kawamura, K., Anlauf, K. G., and Barrie, L. A.: Fine and coarse modes of dicarboxylic acids in the Arctic aerosols collected during the Polar Sunrise Experiment 1997, J. Geophys. Res., 108(D18), 4575, doi:10.1029/203JD003646, 2003.
Narukawa, M., Kawamura, K., Takeuchi, N., and Nakajima, T.: Distribution of dicarboxylic acids and carbon isopotic compositions in aerosols from 1997 Indonesian forest fires, Geophys. Res. Lett., 26, 3101–3104, 1999.
NBSC, National Bureau of Statistics of China: Bulletin of Statistics for Beijing, Part Two: Population, People life and social security, http://www.stats.gov.cn/tjsj/ndsj/2008/indexeh.htm, 2009a.
NBSC, National Bureau of Statistics of China: Bulletin of Statistics for Beijing, Part Three:

Resource, Energy and Environment, http://www.stats.gov.cn/tjsj/ndsj/2008/indexeh.htm, 2009b.
Ohta, S. and Okita, T.: A chemical characterization of atmospheric aerosol in Sapporo, Atmos. Environ., 24A, 815–822. 1990.
Pakkanen, T. A., Kerminen, V. M., Hillamo, R. E., Makinen, M., Makela, T., and Virkkula, A.: Distribution of nitrate over sea-salt and soil derived particles implications from a field study, J. Atmos. Chem., 24, 189–205, 1996.
Peng, C. and Chan, C. K.: The water cycles of water soluble organic salts of atmospheric importance, Atmos. Environ., 35, 1183–1192, 2001.
Seinfeld, J. H. and Pandis, S. N.: Atmospheric Chemistry and Physics-from Air Pollution to Climate Change, John Wiley & Sons, Inc., New York, 1998.
Shao, M., Tang, X. Y., Zhang, Y. H., and Li, W. J.: City clusters in China: air and surface water pollution, Front. Ecol. Environ., 4(7), 353–361, 2006.
Slanina, J., ten Brink, H. M., Otjes, R. P., Even, A., Jongejan, P., Khlystov, A., Waijers-Ijpelaan, A., Hu, M., and Lu, Y.: The continuous analysis of nitrate and ammonium in aerosols by the steam jet aerosol collector (SJAC): extension and validation of the methodology, Atmos. Environ., 35, 2319–2330, 2001.
Stelson, A. W. and Seinfeld, J. H.: Thermodynamic prediction of the water activity, NH_4NO_3 dissociation-constant, density and refractive index for the NH_4NO_3-$(NH_4)_2SO_4$-H_2O system at 25-degrees-C, Atmos. Environ., 16(10), 2507–2514, 1982.
Sun, Y. L., Zhuang, G. S., Tang, A. H., Wang, Y., and An, Z. S.: Chemical characteristics of $PM_{2.5}$ and PM_{10} in haze-fog episodes in Beijing, Environ. Sci. Technol., 40(10), 3148–3155, 2006.
van Pinxteren, D., Brueggemann, E., Gnauk, T., Iinuma, Y., Mueller, K., Nowak, A., Achtert, P., Wiedensohler, A., and Herrmann, H.: Size- and time-resolved chemical particle characterization during CAREBeijing-2006: different pollution regimes and diurnal profiles, J. Geophys. Res., 114, D00G09, doi:10.1029/2008JD010890, 2009.
Wang, L. T., Hao, J. M., He, K. B., Wang, S. X., Li, J. H., Zhang, Q., Streets, D. G., Fu, J. S., Jang, C. J., Takekawa, H., and Chatani, S.: A modeling study of coarse particulate matter pollution in Beijing: regional source contributions and control implications for the 2008 summer Olympics, J. Air Waste Manage., 58(8), 1057–1069, 2008.
Yang, F., He, K., Ye, B., Chen, X., Cha, L., Cadle, S. H., Chan, T., and Mulawa, P. A.: One-year record of organic and elemental carbon in fine particles in downtown Beijing and Shanghai,

Atmos. Chem. Phys., 5, 1449–1457, 2005, http://www.atmos-chem-phys.net/5/1449/2005/.

Yao, X. H., Chan, C. K., Fang, M., Cadle, S., Chan, T., Mulawa, P., He, K. B., and Ye, B. M.: The water-soluble ionic composition of $PM_{2.5}$ in Shanghai and Beijing, China, Atmos. Environ, 36(26), 4223–4234, 2002.

Yao, X. H., Lau, A. P. S., Fang, M., Chan, C. K., and Hu, M.: Size distributions and formation of ionic species in atmospheric particulate pollutants in Beijing, China: 1 – inorganic ions, Atmos. Environ., 37(21), 2991–3000, 2003.

Zhuang, H., Chan, C. K., Fang, M., and Wexler, A. S.: Formation of nitrate and non-sea-salt sulfate on coarse particles, Atmos. Environ., 33, 4223–4233, 1999.

Table 1. Compare of PM_{10}, $PM_{1.8}$, ratios of $PM_{1.8}/PM_{10}$ and $SNA/PM_{1.8}$ with other study ($\mu g/m^3$). SNA: mass sum of (SO_4^{2-}+NO_3^-+NH_4^+).

Site	PM_{10}	$PM_{1.8}$	$PM_{1.8}/PM_{10}$	$SNA/PM_{1.8}$	Year-month	reference
PKU	113.0±55.8	52.0±35.3	0.44±0.13	0.35±0.17	2001-7	Hu, 2005a
PKU	130.9±87.2	70.4±56.5	0.51±0.12	0.55±0.19	2002-7	Hu, 2005a
PKU	171.5±91.4	99.8±74.4	0.64±0.08	0.53±0.19	2006-8	This study
Yufa	111.6±73.2	78.2±58.4	0.76±0.08	0.58±0.18	2006-8	This study

Table 2. PMF resolved average particle concentrations for each mode at two sites during the "polluted" episodes. A: morning, P: afternoon, N: night ($\mu g/m^3$).

	PMF-resolved Yufa average			PMF-resolved PKU average			
	condensation	droplet	coarse	condensation	droplet-1	droplet-2	coarse
Mass-A	26.34	58.18	24.22	13.88	81.77	23.89	59.73
Mass-P	28.51	52.46	22.48	6.57	103.79	24.92	71.29
Mass-N	29.47	53.59	26.45	7.53	54.74	28.74	65.85
SO_4^{2-}-A	6.33	21.65	3.11	3.44	14.18	9.84	0.88
SO_4^{2-}-P	9.06	26.43	1.80	5.60	17.55	10.36	2.47
SO_4^{2-}-N	4.40	19.11	1.92	4.29	10.99	9.47	2.61
NO_3^--A	1.95	7.05	3.25	0.50	1.88	9.94	10.54
NO_3^--P	0.32	2.45	5.05	0.73	2.53	8.69	11.04
NO_3^--N	2.37	9.22	2.72	0.35	5.89	7.41	5.42

ACPD
9, 23955–23986, 2009

Table 3. Linear regressions between the cations and nitrate in fine particles in the afternoon samples at PKU, using $y=bx+c$, in which y represents molar concentration of Na^+, K^+ or twice Ca^{2+}, x molar concentration of nitrate.

Regress coefficients	1–1.8 μm				0.56–1 μm			
	Na^+	K^+	2^*Ca^{2+}	$K^++2^*Ca^{2+}$	Na^+	K^+	2^*Ca^{2+}	$K^++2^*Ca^{2+}$
b	0.17	0.37	0.9	0.99	0.17	0.42	0.23	0.6
c	0.0016	0.0009	−0.0006	0.0033	0.0012	0.001	0.0013	0.0029
R^2	0.61	0.78	0.94	0.97	0.72	0.9	0.97	0.95

ACPD
9, 23955–23986, 2009

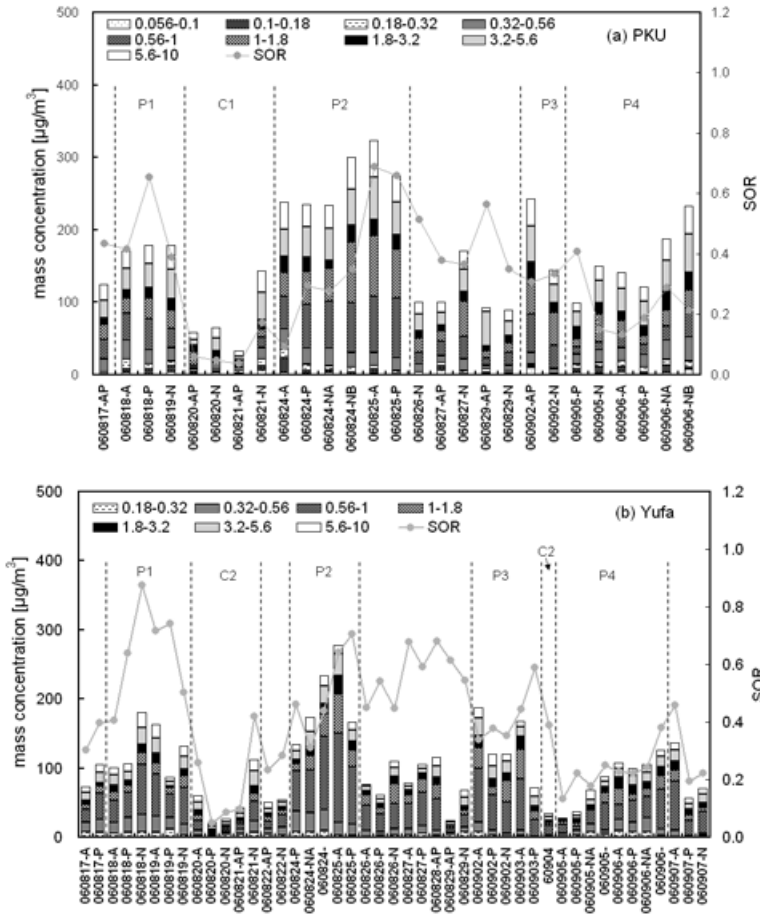

Fig. 1. PM_{10} and size-segregated particle mass concentrations for each sample during the campaign. **(a)** PKU, **(b)** Yufa.

ACPD
9, 23955–23986, 2009

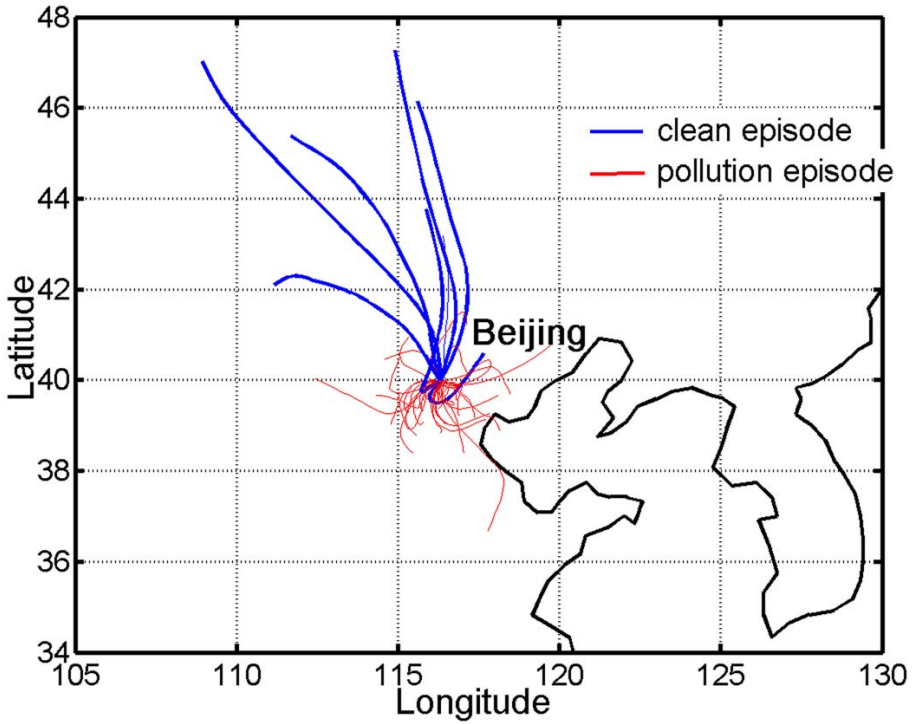

Fig. 2. 24 h backward trajectories during the campaign. Two backward trajectories per day with the starting time at 12:00 and 24:00, at the starting height of 100 m.

ACPD
9, 23955–23986, 2009

Title Page
Abstract Introduction
Conclusions References
Tables Figures
◀I ▶I
◀ ▶
Back Close
Full Screen / Esc
Printer-friendly Version
Interactive Discussion

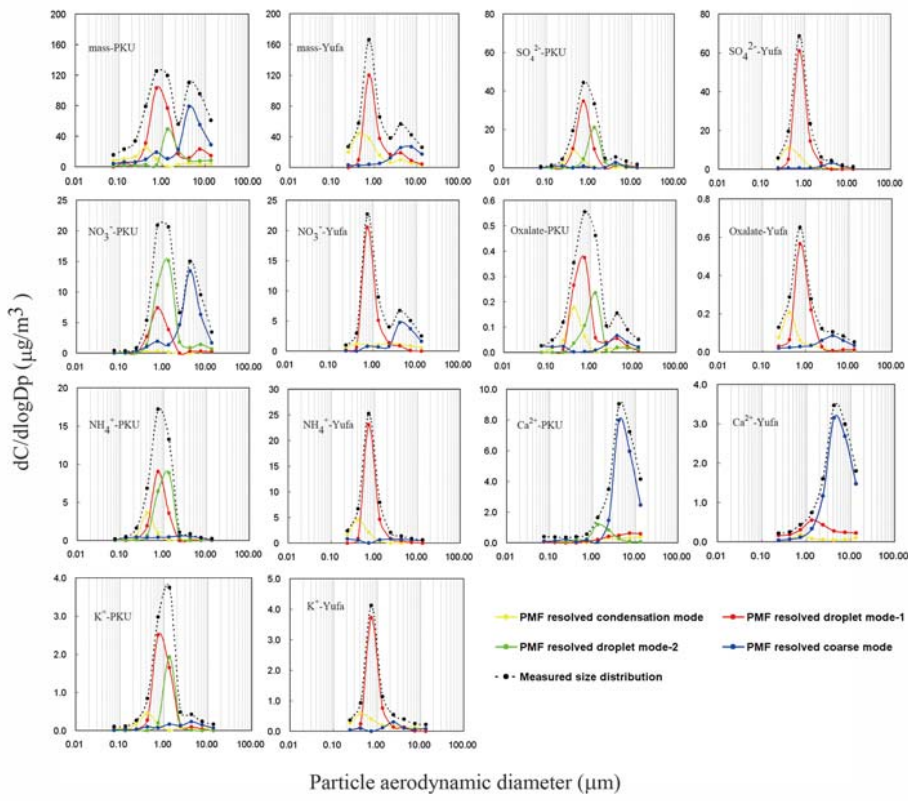

Fig. 3. The average measured size distribution curves and the PMF resolved four-modal or three-modal curves for the mass and major ionic species.

ACPD
9, 23955–23986, 2009

Title Page
Abstract Introduction
Conclusions References
Tables Figures
◀I ▶I
◀ ▶
Back Close
Full Screen / Esc
Printer-friendly Version
Interactive Discussion

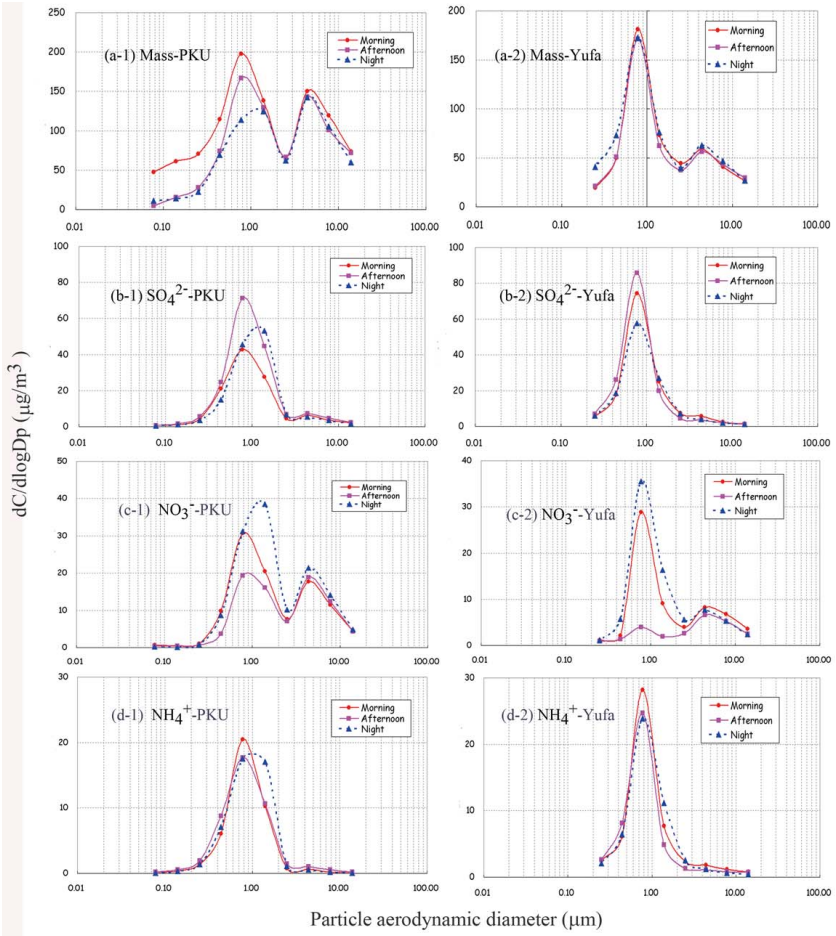

Fig. 4. Measured average size distributions of mass and major secondary ionic compounds for morning, afternoon and night samples.

ACPD
9, 23955–23986, 2009

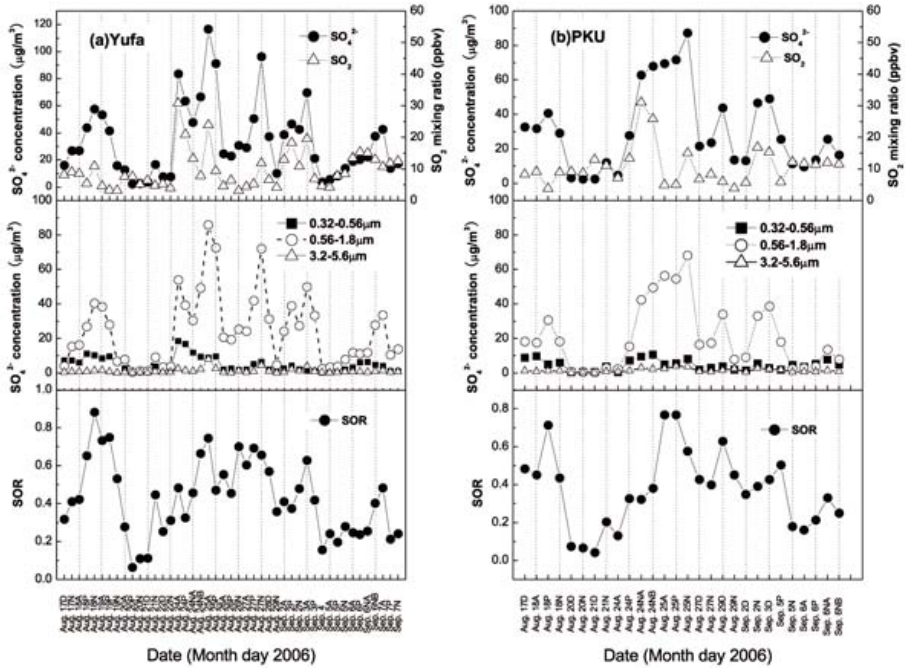

Fig. 5. Concentrations of total and size-resolved SO_4^{2-} along with corresponding SO_2 mixing ratios and SOR at Yufa and PKU site. SOR is defined as the molar ratio of the SO_4^{2-} to the total sulfur ($SO_4^{2-}+SO_2$), **(a)** Yufa, **(b)** PKU.

ACPD
9, 23955–23986, 2009

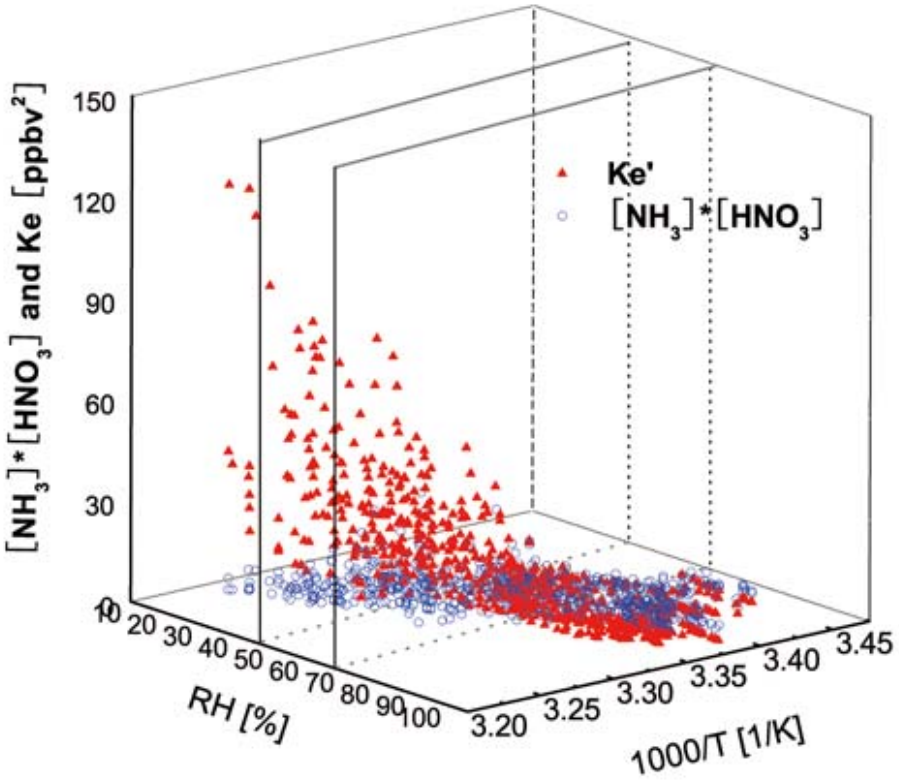

Fig. 6. Equilibrium constant (Ke′) and measured $[NH_3]\times[HNO_3]$ at PKU during the campaign. Red triangles for Equilibrium constant Ke′, blue circles for measured $[NH_3]\times[HNO_3]$, rectangles for RH=50%, 70%.

ACPD
9, 23955–23986, 2009